Position-Dependent Local Motions in Spin-Labeled Analogues of a Short α-Helical Peptide Determined by Electron Spin Resonance†

Siobhan M. Miick, A. Paul Todd, and Glenn L. Millhauser*
Department of Chemistry and Biochemistry, University of California, Santa Cruz, California 95064
Received April 16, 1991; Revised Manuscript Received July 18, 1991

ABSTRACT: We have used electron spin resonance and circular dichroism to examine and compare the dynamics in two analogues of the Ala-based 3K(I) peptide [Marqusee, S., Robbins, V. H., & Baldwin, R. L. (1989) *Proc. Natl. Acad. Sci. U.S.A. 86*, 5286–5290], labeled at positions 4 and 8, throughout the α-helix → coil transition. In the middle of the thermal unfolding transition, our results demonstrate that the local mobility near the N-terminus is greater than at the center of the peptide. This provides evidence, from the perspective of dynamics, that the ends of Ala-based α-helices are frayed. We further find that the position dependence of the mobility for the thermally unfolded state differs from that of the denaturant unfolded state. Only the latter state exhibits the local dynamics expected for a genuine random coil.

There has been a recent revolution in structural biochemistry following from the discovery of short helical peptides (16-mers and 17-mers) of very high α-helical content (≥70%) (Marqusee & Baldwin, 1987; Marqusee et al., 1989). Previously, it had been generally predicted that short peptides (less than 20 residues) would not be helical. (Rare exceptions to these predictions included the C- and S-peptide fragments of ribonuclease A, which exhibit a fractional helicity on the order of 25% at 1 °C.) These initial results have spawned a new field of research into the origin of this anomalously high helical content. The common theme among these helical peptides is that they contain mainly alanine (Ala), which is the simplest chiral amino acid. It appears now that Ala has a much higher α-helix-forming tendency than previously thought and that short soluble peptides with a large percentage of alanine will form helices (Padmanabhan et al., 1990; Merutka et al., 1990).

A physical understanding of protein folding is a central goal of modern biochemistry. α-Helices are the most common form of secondary structure in proteins, and the discovery of these helical peptides offers the exciting opportunity of exploring the structure, dynamics, and folding of short helices in isolation. Among the first pressing questions in this regard is to determine exactly how the helicity is distributed in these short peptides. Do all of the residues share the same degree of helicity or is the helicity more concentrated in certain regions such as the middle of the peptide? This issue was recently addressed in a study where analogues of the 3K(I) α-helical peptide (Ac-AAAAKAAAAKAAAAKA-NH_2) were synthesized each with a single Ala → Gly substitution (Chakrabartty et al., 1991). If Gly, a strong helix breaker, is placed in a region of the peptide that is mainly coil, the measured helicity of the peptide will remain unchanged. In contrast, if the Gly is placed in a helical region of the peptide, the helicity will be reduced. By this method, it was shown that helicity is mainly concentrated in the central region of the peptide and the peptide ends are frayed.

The position dependence of peptide helicity has also been addressed by two recent NMR investigations. In one study, helical 17-mers were designed each with a very heterogeneous sequence to avoid overlapping NMR resonances (Bradley et al., 1990). Position-dependent NOE's and three-bond coupling constants demonstrated that helicity was mainly concentrated in the central region of the peptide between residues 5 and 15. Helicity in this region was estimated to be approximately 80%. In a second study, researchers constructed a class of helical peptides with the sequence succinyl-$YSE_4K_4X_3E_4K_4$-NH_2, in which X is a guest residue (Liff et al., 1991). Helicity in this peptide is stabilized by Glu^-···Lys^+ salt bridges, and this is qualitatively different from the 3K(I), for example, which is stabilized by the helix-forming tendency of Ala. Helicity was evaluated with three different structure-sensitive techniques: NOE's, three-bond coupling constants, and the chemical shift of the C_α protons. All three experiments indicated that helicity is skewed toward the N-terminus with a maximum at position 8.

There is another means of testing for local structure in peptides: measurement of the local dynamics. Helical regions of peptides are hydrogen bonded and are expected to be more rigid than coil regions. Thus, a measure of local dynamics as a function of position would yield information complementary to that described above. We recently reported an electron spin resonance (ESR) spin label technique that we developed to probe both local and global peptide dynamics (Todd & Millhauser, 1991).[1] We showed that a short helical peptide could be spin labeled in a site-specific fashion with little change in the helical character as determined by circular dichroism (CD). Site-specific labeling was accomplished by replacing an Ala with a Cys followed by labeling at the Cys with methanethiosulfonate nitroxide spin label (MTSSL). We further showed that, in the low-temperature α-helical regime, motion of the spin label relative to the peptide was slow compared to the rotational correlation time of the labeled peptide. ESR line shapes in this regime, therefore, reflect mainly the overall tumbling of the peptide. Using temperature variation, we gathered ESR spectra throughout the α-helix → coil transition, with only nanomole quantities of peptide, and we interpreted our results using the concept of a local tumbling volume V_L (see below). In the high-temperature regime, which favors the coil state of the peptide, we found that V_L decreased significantly when compared to the α-helix

†This work was supported by a grant from the National Science Foundation (DMB-8916946). Portions of this work were also supported by faculty research funds granted by the University of California, Santa Cruz. Acknowledgment is made to the donors of The Petroleum Research Fund, administered by the American Chemical Society, for partial support of this research.

[1] We will refer to this previous study as T&M.

0006-2960/91/0430-9498$02.50/0

regime, and this was readily interpreted in terms of an increased flexibility of the peptide backbone at the nitroxide attachment point.

In this report, we apply our recently developed technique to examine and compare two spin-labeled analogues of the α-helical 3K(I) peptide, which are shown here along with their designations:

Ac-AAACKAAAAKAAAAKA-NH_2 3K-4

Ac-AAAAKAACAKAAAAKA-NH_2 3K-8

The 3K-4 and 3K-8 peptides differ from the 3K(I) (Marqusee et al., 1989) only in the Ala → Cys substitution at positions 4 and 8, respectively. The 3K(I) peptide is helical because of the many Ala residues, and the Lys^+ serve to confer solubility in aqueous solution.

Our rationale for the choice of labeling positions in these peptide analogues is as follows. Comparison of the 3K-8 with the 3K-4 provides a view of how structure and dynamics differ between the middle position and a position near the end of an α-helix. For testing end effects, we chose to label position 4 because positions 1–3 cannot completely hydrogen bond when the peptide is in an α-helical configuration. (Note: When the amino-terminus is blocked with an acetyl group, the amino acid at position four can hydrogen bond with this acetyl group.) We are most interested in flexibility that arises in residues that can potentially form the same number of hydrogen bonds as the more central regions of the α-helix. Also, in an α-helix, there can be steric interactions between side chains that are spaced i+4 residues away from each other. Therefore, to insure uniformity of such interactions, we have placed the Cys in both of the peptides so that there is an Ala i+4 positions away.

We explore the temperature dependent CD and ESR of the two peptides. By combining results from these two techniques, we probe variations in local and global structure throughout the α-helix → coil transition. As mentioned, ESR line shapes reflect both the global reorientation of the various spin-labeled peptides and local peptide backbone motion at the nitroxide attachment point. The correlation times for global reorientation are less than a nanosecond for these short peptides. However, if there is additional local motion at the nitroxide attachment point, also on the nanosecond time scale, then parameters extracted from the ESR line shapes will reflect this. Our experiments suggest that such motions are greater near the helix ends, and these results lend considerable support, from the perspective of dynamics, to the apparent fraying of the helical ends as outlined above. In addition to this, we are able to directly probe differences in position-dependent mobilities in both aqueous solution and in denaturant. We find that the thermally unfolded random coil state of these peptides, in water, does not exhibit the characteristic mobility profile expected for a free chain polymer in solution.

Materials and Methods

Peptide Synthesis and Spin Labeling. The two 3K peptides were custom synthesized by the American Peptide Co. Methanethiosulfonate spin label (MTSSL) (Berliner et al., 1982) was obtained from Reanal (Budapest, Hungary). Peptides were labeled with MTSSL according to the following reaction.

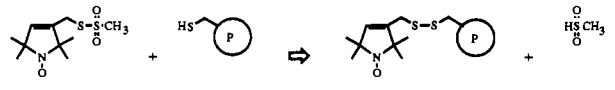

Purification by HPLC and characterization have been previously described in T&M. All experiments were performed with buffer conditions of 50 mM sodium phosphate at pH 7 (except where noted). Concentrations for CD and ESR measurements were determined from double integration of the ESR spectrum followed by comparison with a standard aqueous 1.0 mM 4-hydroxy-TEMPO solution. Concentrations determined in this manner are accurate to better than 5%. Following variable temperature ESR or CD, samples were checked for any degradation by HPLC.

Circular Dichroism. CD spectra were acquired with an AVIV 60DS circular dichroism spectrometer calibrated with (+)-10-camphorsulfonic acid. Samples contained 100 μM peptide in the buffer described above.

Electron Spin Resonance. ESR spectra were acquired with a Bruker ESP 380 spectrometer operated in continuous wave (CW) mode with a TE_{102} rectangular cavity and a variable temperature accessory. Samples (20 μL) of 1.0–1.5 mM peptide were contained in sealed glass micropipets. To avoid line shape distortion, the modulation amplitude was set to 0.2 G, which was always less than one-fifth of the first-derivative peak-to-peak line width.

Extraction of τ_R and V_L from ESR Spectra. In T&M we reviewed, in detail, the determination of rotational correlation times (τ_R) from ESR spectra. In that study of an analogue of the i+4 (E,K) peptide (Marqusee & Baldwin, 1987), we determined that the motional anisotropy was small and nearly constant throughout the α-helix → coil transition. We further argued that it would be difficult to quantify the degree of anisotropy without highly accurate hyperfine tensor values, which are not presently available. Thus, rotational diffusion in T&M was modeled in terms of isotropic motion. Using the same methods, we have also analyzed the ESR spectra of the 3K peptides (data not shown). Again we find there is little indication of highly anisotropic reorientation, so we interpret the data in this present study in terms of isotropic rotational diffusion. For a careful discussion of these matters, we refer the reader to T&M. Below we briefly review the essential points for the extraction of isotropic rotational correlation times and local volumes (V_L).

In the motionally narrowed regime (τ_R < 2 ns), the homogeneous line width $T_2(M)^{-1}$ of the Mth hyperfine line in a nitroxide spectrum is described by

$$T_2(M)^{-1} = A + BM + CM^2 \quad (1)$$

The line shape parameter B can be used to determine τ_R and is readily determined from the spectra with the relation

$$B = \frac{\sqrt{3}}{4}\Delta H(0)\left[\sqrt{\frac{V(0)}{V(+1)}} - \sqrt{\frac{V(0)}{V(-1)}}\right] \quad (2)$$

where $V(M)$ is the peak-to-peak height of the Mth line in a first-derivative ESR spectrum and $\Delta H(0)$ is the peak-to-peak width of the M = 0 hyperfine line. In the presence of heterogeneous line broadening, B requires minor corrections, and the technique for this has been described in T&M. τ_R is related to B with the relation

$$B = \frac{\pi}{10}\omega_0[g^{(0)}D^{(0)}[(16/3)j_0(0) + 4j_0(\omega_0)] + 2g^{(2)}D^{(2)}[(16/3)j_2(0) + 4j_2(\omega_0)]] \quad (3)$$

where $j_m(\omega)$ are the spectral densities

$$j_m(\omega) = \frac{\tau_R}{1 + \tau_R^2\omega^2} \quad (4)$$

and ω_0 is the Larmor frequency. In the range of correlation times covered in this study, the spectral density at $\omega = \omega_0$ can be approximated by $j_m(\omega) = 0$. The spherical tensor com-

ponents, $g^{(m)}$ and $D^{(m)}$, are determined from the principal values of the MTSSL **g** and **A** tensors. We use the same values of **g** and **A** for MTSSL as were used in T&M.

Dynamic processes that symmetrically shorten the T_2 of all three hyperfine lines affect only the A line shape parameter of eq 1. Such relaxation mechanisms include spin exchange between labeled peptides and nitroxide collisions with dissolved O_2. The parameter B, which we use to determine τ_R, should not be affected by such processes. To ensure experimentally that B would not be affected by variations in peptide concentration or small amounts of dissolved O_2, we performed two series of experiments (data not shown). In the first series, we examined the values of B vs peptide concentration at five different temperatures. To within experimental error, no variation in B with concentration was observed. In the second series we bubbled He through our solvents, before peptide was added, to remove O_2. We compared B values from these deoxygenated samples to samples where O_2 was not removed, and again no variation in B was observed. These findings are consistent with the theoretical expectation that B is not affected by symmetric line-broadening mechanisms. Thus, in the samples used in this study we did not further attempt to remove dissolved O_2.

As we have shown in T&M, direct interpretation of τ_R can be difficult in variable temperature experiments because its value is strongly affected by changes in both solution viscosity and temperature. It is more useful, therefore, to develop the concept of a local tumbling volume defined through the Stokes–Einstein (SE) relation for isotropic rotational diffusion

$$V_L = \frac{kT\tau_R}{\eta} \tag{5}$$

where η is the solution viscosity, T is the absolute temperature, and k is Boltzmann's constant. V_L reflects the volume of the peptide that reorients with the nitroxide on the time scale of τ_R. For example, if the spin label is attached to a rigid α-helical peptide, then V_L will correspond to the hydrodynamic volume of the entire helix–label complex. However, if there are local structural fluctuations, then V_L will reflect a hydrodynamic volume less than that expected for the rigid helix–label complex. These fluctuations must occur on a time scale close to the peptide rotational correlation time or less, otherwise the ESR line shapes, and hence V_L, will reflect only the global reorientation process of the spin-labeled peptide. In previous work we showed that $\tau_R < 1$ ns for an analogue of the i+4 (E,K), at all temperatures, and this also holds for the two 3K peptides.

Results

Variable Temperature CD and ESR of Spin-Labeled Peptides. At low temperature, both peptides in this study exhibit CD spectra characteristic of α-helices. The usual measure of helicity is the mean residue ellipticity at 222 nm ($-[\theta]_{222}$) [see, for example, Padmanabhan et al. (1990)]. In Figure 1 we show $-[\theta]_{222}$ vs temperature for the spin-labeled peptides. Qualitatively, both of the peptides exhibit the same behavior, the helicity is greatest at the lowest temperature (1 °C) and monotonically decreases as the temperature is increased. The 3K(I) parent peptide exhibits this same type of temperature dependence (Marqusee et al., 1989) although the 3K-8 and 3K-4 appear to have a slightly higher $-[\theta]_{222}$ than the 3K(I) at 1 °C (274 K). Comparing our results with the 3K(I), we estimate that the fractional helicity of these spin-labeled analogues is between 70% and 85%.

On closer inspection, there are resolvable differences between the curves for the 3K-8 and the 3K-4 peptides. At the high

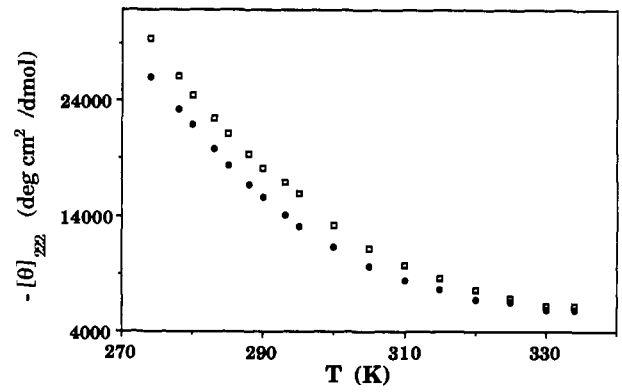

FIGURE 1: $-[\theta]_{222}$ vs temperature for the peptides 3K-4 (□) and 3K-8 (●).

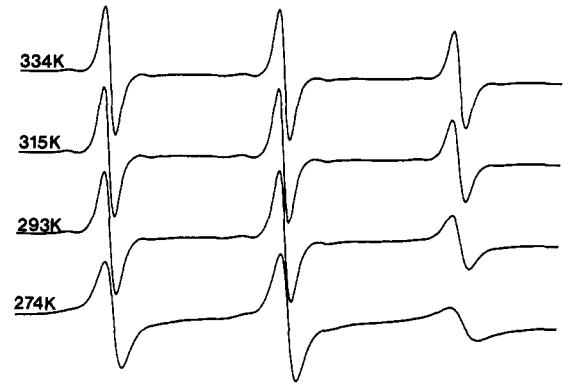

FIGURE 2: Temperature-dependent ESR spectra (50-G scan) of the 3K-8 peptide at pH 7.

end of the temperature range, the two curves superimpose. However, as the temperature is lowered, the 3K-4 peptide reaches a somewhat higher value of $-[\theta]_{222}$ than 3K-8 by about 10%. This difference is reproducible and greater than the experimental error (due to concentration variations) of 5%. The slightly lowered helicity of the 3K-8 peptide over 3K-4 may indicate that the substitution Ala → Cys-MTSSL creates a small, but measurable, perturbation of the α-helical structure when in the center of the peptide. In turn, this suggests that the helicity is greater in the helix center, and this has been shown in studies of systematic Gly substitutions (Chakrabartty et al., 1991).

The ESR spectra, and the computed values for V_L, are strongly temperature dependent. Spectra for the 3K-8 peptide at four temperatures are shown in Figure 2. As the temperature is lowered the hyperfine lines broaden, and this is especially pronounced in the high field line ($M = -1$). Using the methods described above, we have extracted the temperature-dependent values for V_L, and these are shown for both peptides in Figure 3. These values were measured in triplicate and averaged to reduce the random error to less than 1.5%. Through the low-temperature region, from 274 to 295 K, data were gathered in alternating 2 and 3K intervals. Above 295 K, data were gathered at 5 K intervals. Both peptides exhibit the same overall qualitative behavior. At the low end of the temperature range, the V_L's reach a maximum with values between 1900 and 2000 Å^3. An α-helix has a radius of approximately 5 Å and a pitch of 1.49 Å/residue, and so a completely hydrogen-bonded 16-mer has an expected hydrated volume of approximately 2000 Å. Thus, these α-helices appear to tumble as nearly rigid units at 274 K. As T is raised, V_L decreases, indicating the onset of localized motions. Whereas an α-helix is characterized by a rigid structure, the coil state appear to allow for localized motions of the peptide backbone.

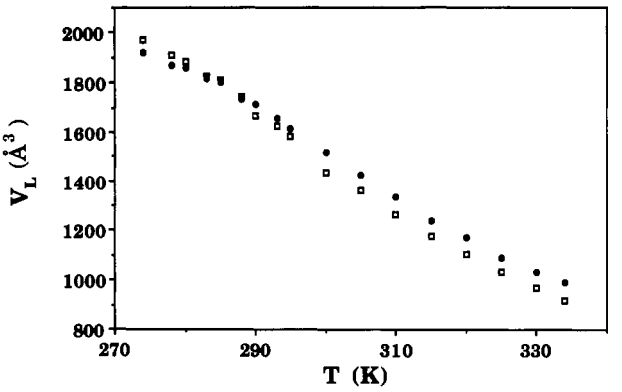

FIGURE 3: V_L vs temperature for the peptides 3K-4 (□) and 3K-8 (●).

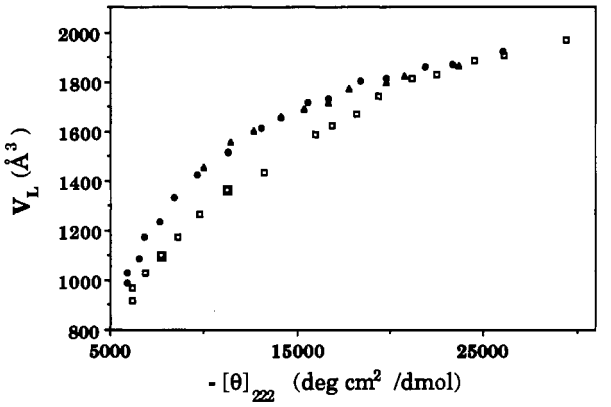

FIGURE 4: V_L vs $-[\theta]_{222}$ for the peptides 3K-4 (□) and 3K-8 (●), which shows that local motion is more pronounced at position 4 as the helicity is lowered. Data are also shown for the 3K-8 peptide at pH 2 (▲).

Comparison of the 3K-4 and 3K-8 peptides reveals position-dependent dynamics. Simple inspection of the two curves of Figure 3 indicates that local motion sensed at the two different attachment points exhibit different temperature dependences. At the low end of the temperature range, V_L for the 3K-4 [i.e., V_L(3K-4)] is greater than V_L(3K-8). As the temperature is raised, the two curves cross near 290 K, and at all higher temperatures the 3K-8 curve is above the 3K-4 curve. These trends are well resolved and substantially greater than the experimental random error. The stronger temperature dependence of V_L(3K-4), compared to V_L(3K-8), along with V_L(3K-4) < V_L(3K-8) at higher temperatures, indicates that there is greater nanosecond flexibility near the amino-terminus.

V_L vs $-[\theta]_{222}$: Position-Dependent Local Motions in the 3K Peptides. In this study, temperature is used mainly to tune the degree of fractional helicity of our labeled peptides. However, direct comparison of the two peptides, at a particular temperature, is hindered because the two peptides will probably have different values of $-[\theta]_{222}$. It is useful, therefore, to plot V_L vs $-[\theta]_{222}$, and this is done for the two 3K peptides in Figure 4. Such a plot allows for a direct examination of local dynamics as a function of helicity. It should be noted, however, that for each point along the $-[\theta]_{222}$ axis the two peptides will be at slightly different temperatures although the difference in T will always be less than 5 °C.

At high helicity the behavior of the two peptides is nearly identical. This makes sense because two points on a nearly rigid helix will both reorient with the helix and have the same V_L's. As the helicity is lowered to about halfway through the transition, around $-[\theta]_{222} \approx 14000$, V_L(3K-4) drops well below V_L(3K-8). This lower V_L for the 3K-4 again indicates that

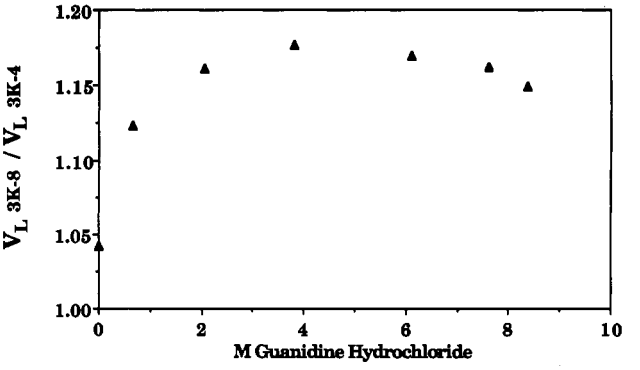

FIGURE 5: Ratio of the V_L's for the peptides 3K-8 and 3K-4 vs [Gu·HCl]. Data were collected at 298 K. The ratio at [Gu·HCl] > 4 M is consistent with that expected for a random coil.

there is more flexibility at the N-terminus of the peptide than the middle of the peptide. Figure 4 also indicates that as the helicity is lowered even farther, near $-[\theta]_{222} \approx 6000$, the 3K-4 and 3K-8 curves approach each other and that V_L(3K-8) is greater than V_L(3K-4) by approximately 8% [i.e., V_L(3K-8)/V_L(3K-4) = 1.08]. This suggests that the local dynamics in the coil state do not exhibit as strong a position dependence as found near the middle of the transition.

We found this high-temperature result to be surprising because it is well known that ideal free polymers in solution exhibit greater flexibility near the polymer termini (Doi & Edwards, 1986) and, therefore, we expected that the 3K-8 curve would be well above the 3K-4 curve at low helicity. We further explored this by using the denaturant guanidine hydrochloride (Gu·HCl) to induce the random coil state in the two peptides. It has been shown that the 3K(I) is partially denatured, to $-[\theta]_{222} \approx 4{,}000$, when [Gu·HCl] ≈ 4 M (Marqusee et al., 1989). Our results at 298 K are shown in Figure 5. We plot the ratio of the V_L's to eliminate any error introduced by changes in the solution viscosity as guanidine is added. (Note that local dynamics in polymers are often described in terms of correlation times. The ratio of the V_L's is equivalent to the ratio of the τ_R's because of their direct proportionality from the SE equation.) In the absence of the denaturant, V_L's for the middle and the end of the partially helical peptide have a ratio of 1.04. As guanidine is added, beyond [Gu·HCl] = 2 M, the ratio of the V_L's increases to approximately 1.18, indicating that V_L(3K-8) is greater than V_L(3K-4) by about 18%, in turn, indicating greater mobility at the end of the peptide. This now shows a much stronger position dependence than the thermally unfolded species. These results in Gu·HCl are quantitatively consistent with the theoretical predictions for a free chain polymer in solution (see below).

We have also investigated the pH dependence of the V_L vs $-[\theta]_{222}$ curve for the 3K-8. CD studies have indicated that the helicity is not effected by a lowering of the pH and no effect is expected as long as the lysine residues retain their positive charge. Our data, shown in Figure 4, superimpose on the data for the 3K-8 at pH 7. (Only the low-temperature data were gathered because at high temperature and low pH we have found that there is slight decomposition of the spin-labeled peptides.) Thus, we find that low pH does not impact the local dynamics at position 8.

Discussion

The results in both Figures 3 and 4 clearly show that, in the partially unfolded 3K(I) helical peptide, local motion is more pronounced at the N-terminus than in the middle of the

peptide. This, in turn, lends support to the discovery that the ends of short helical peptides are frayed (although we have not yet examined local motions near the C-terminus). In the interpretation of our results, one might be concerned with the influence of the Ala → Cys-MTSSL substitution on the local helicity at the substitution point in the peptide sequence. We believe that there are two issues to consider here. First, we have shown that 3K peptides with this substitution are still very helical and compare quantitatively with the 3K(I) peptide. This is consistent with the finding that hydrophobic residues without β-branching are strong α-helix formers (Padmanabhan et al., 1990; see also the discussion in T&M). Thus, the Cys-MTSSL "residue" behaves similarly to an Ala or a Leu, and, likewise, the α-helicity at the nitroxide label point should be relatively unchanged when compared to an analogous peptide with an Ala or Leu in the same position. Second, even if spin labeling changed the local helicity, one would expect such a change to occur regardless of the location of the label in the sequence. If this local distortion dominated the local motion, then the difference in local motion is measured by the nitroxide would become independent of label location. Nevertheless, we clearly do observe position-dependent local motions so the Cys-MTSSL "residue" must provide a good measure of these local dynamics.

When comparing our results with other work on this subject, such as that outlined in the introduction, it is important to distinguish the physical basis of our particular measurements. The work on Gly-substituted 3K(I) analogues provides a thermodynamic perspective; interpretations hinge upon changes in the helix → coil equilibrium in response to the site-specific introduction of a helix-breaking residue. In contrast, NMR studies on short helical peptides provide a structural perspective in the identification of local helical domains. We have now added the perspective of local dynamics. Thus, thermodynamic measurements, structural measurements, and now measurements of local dynamics all consistently indicate that the ends of short helices are frayed. Furthermore, our experiments provide a comparison of local dynamics as a function of fractional helicity, so the emergence of the frayed ends can be followed through the α-helix → coil transition.

We find that the difference in local dynamics, between positions 4 and 8, is greatest near the middle of the α-helix → coil transition where $-[\theta]_{222} \approx 14\,000$. At both positions there is local motion, as indicated by the general decrease in V_L; however, this decrease is more pronounced at position 4. We can estimate the time scale of the additional local motions at position 4, although it is difficult to be completely quantitative without knowledge of the amplitude and the anisotropy of these local motions. Nevertheless, we argue that the motion sensed at position 4 should be similar to that at position 8, except that there is an additional flexibility from fraying near the N-terminus of the α-helix. To a first approximation, the reciprocals of correlation times are additive, and so the observed motion at position 4 is given by

$$\frac{1}{\tau_R(\text{3K-4})} = \frac{1}{\tau_R(\text{3K-8})} + \frac{1}{\tau_R(\text{loc})} \qquad (6)$$

where τ_R(3K-4) and τ_R(3K-8) are the rotational correlation times measured by the nitroxide at the two positions and τ_R(loc) is the correlation time for additional local motions at position 4. From this we find $\tau_R(\text{loc}) \approx 3$ ns when $-[\theta]_{222} \approx 14000$. Thus, near the middle of the α-helix → coil transition, position 4 experiences additional motions, when compared to position 8, and the correlation time for this motion is several nanoseconds. It is interesting to note that the rate constant for the formation of hydrogen bonds in α-helices (k_f) has been determined to fall in the range 10^8–10^{10} s^{-1} in aqueous solution with the most recent measurement giving $k_f = 5.6 \times 10^9$ s^{-1} (Gruenwald et al., 1979). This, in turn, corresponds to a lifetime for hydrogen bonds of somewhat less that 1 ns. It is quite possible that the additional local motion at the N-terminus, sensed in our experiments, corresponds to a flickering formation and breakage of hydrogen bonds in the α-helix framework.

The structure of the random coil state is of critical importance for the understanding of protein folding. Our results at low $-[\theta]_{222}$ suggest that the coil state is flexible, as indicated by the overall decrease in V_L for both 3K peptides. However, there is only a small position dependence of the local dynamics, which is not the expected behavior for a random coil in solution. In fact, hydrodynamic calculations on random coil 50-mers of polyalanine were performed (Perico, 1989), and, if these results are extrapolated to the case of a 20-mer, the calculations predict that position 4 will be approximately 20% more mobile than position 8 (i.e., V_L(3K-8)/V_L(3K-4) ≈ 1.2). Our results in Gu·HCl are consistent with this mobility profile, whereas our results in aqueous solution clearly are not. Thus, our experiments indicate that the thermally unfolded state (i.e., no denaturant) does not exhibit the characteristics of a genuine random coil as calculated by Perico. We believe that this nonhelical species is flexible but definitely not extended as a free chain would be. It is quite possible that a more compact or hydrophobically collapsed species is more consistent with the mobility profile revealed by our experiments. Furthermore, it is well documented for proteins that thermal denaturation and Gu·HCl denaturation lead to different unfolded states (Tanford, 1968). Hydrodynamic measurements of proteins in concentrated Gu·HCl are consistent with that theoretically expected for a random coil state. In contrast, thermally unfolded proteins retain elements of their folded structure. Our results suggest that these two different folding characteristics are maintained in simple α-helical peptides that contain only a single element of secondary structure and no tertiary structure whatsoever.

Finally, computer molecular dynamics techniques are just now on the threshold of calculating protein dynamics and unfolding for α-helices on the nanosecond time scale (Soman et al., 1991; Tirado-Rives & Jorgensen, 1991). Results from such studies will certainly provide key insights into protein folding. However, the validity of such results rely on experimental studies that can be used for comparison. Because we are able to quantify the time scale for local motions in a model α-helix on the nanosecond time scale, our results should serve as an excellent test for such molecular dynamics studies.

Conclusion

We have used spin label ESR to probe the global and local motions in two analogues of an Ala-based α-helical peptide throughout the α-helix → coil transition. As with our previous work in T&M, we find that the spin label introduces only a minor perturbation of the α-helix structure. Our measurements of position-dependent dynamics clearly indicate that thermal unfolding is more pronounced at the N-terminus than in the center of these short α-helices. We have further shown that the thermally unfolded state and the denaturant unfolded state possess different position-dependent mobilities. The latter state more closely exhibits the motional characteristics consistent with that expected for a genuine random coil.

Acknowledgments

We thank Dr. R. L. Baldwin for comments on the manuscript and for helpful discussions.

REFERENCES
Berliner, L. J., Grunwald, J., Hankovsky, H. O., & Hideg, K. (1982) *Anal. Biochem. 119*, 450-455.
Bradley, E. K., Thomason, J. F., Cohen, F. E., Kosen, P. A., & Kuntz, I. D. (1990) *J. Mol. Biol. 215*, 607-622.
Chakrabartty, A., Schellman, J. A., & Baldwin, R. L. (1991) *Nature 351*, 586-588.
Doi, M., & Edwards, S. F. (1986) *The Theory of Polymer Dynamics*, Clarendon, Oxford.
Gruenwald, B., Nicola, C. U., & Schwarz, G. (1979) *Biophys. Chem. 9*, 137-147.
Liff, M. I., Lyu, P. C., & Kallenbach, N. R. (1991) *J. Am. Chem. Soc. 113*, 1014-1019.
Marqusee, S., & Baldwin, R. L. (1987) *Proc. Natl. Acad. Sci. U.S.A. 84*, 8898-8902.
Marqusee, S., Robbins, V. H., & Baldwin, R. L. (1989) *Proc. Natl. Acad. Sci. U.S.A. 86*, 5286-5290.
Merutka, G., Lipton, W., Shalongo, W., Park, S. H., & Stellwagen, E. (1990) *Biochemistry 29*, 7511-7515.
Padmanabhan, S., Marqusee, S., Ridgeway, T., Laue, T. M., & Baldwin, R. L. (1990) *Nature 344*, 268-270.
Perico, A. (1989) *Biopolymers 28*, 1527-1540.
Soman, K. V., Karimi, A., & Case, D. A. (1991) *Biophys. J. 59*, 397a.
Tanford, C. (1968) *Adv. Protein Chem. 23*, 121-282.
Tirado-Rives, J., & Jorgensen, W. L. (1991) *Biochemistry 30*, 3864-3871.
Todd, A. P., & Millhauser, G. L. (1991) *Biochemistry 30*, 5515-5523.

Structural Basis for the Inactivation of the P54 Mutant of β-Lactamase from *Staphylococcus aureus* PC1†

Osnat Herzberg,*,‡ Geeta Kapadia,‡ Bernardo Blanco,§ Tom S. Smith,§ and Andrew Coulson§

Center for Advanced Research in Biotechnology, Maryland Biotechnology Institute, University of Maryland, 9600 Gudelsky Drive, Rockville, Maryland 20850, and Institute for Cell and Molecular Biology, University of Edinburgh, King's Building, Mayfield Road, Edinburgh EH9 3JR, U.K.

Received May 17, 1991; Revised Manuscript Received July 11, 1991

ABSTRACT: The crystal structure of a mutant protein of a class A β-lactamase from *Staphylococcus aureus* PC1, in which Asp179 is replaced by an asparagine (P54), has been determined and refined at 2.3-Å resolution (1 Å = 0.1 nm). The resulting crystallographic R factor ($R = \sum_h||F_o| - |F_c||/\sum_h|F_o|$, where $|F_o|$ and $|F_c|$ are the observed and calculated structure factor amplitudes) is 0.181 for 12 289 reflections with $I \geq \sigma(I)$ within the 6.0-2.3-Å resolution range. The mutated residue is located at the C-terminus of an extensive loop (the Ω-loop), remote from the active site, and results in a drastically reduced activity. Examination of the native and P54 structures reveals that the overall fold is similar, except that there is substantial disorder of the Ω-loop of P54. This is a consequence of the elimination of a salt bridge between Asp179 and Arg164 that links the two ends of the Ω-loop in native β-lactamase. It is associated with a difference in side-chain conformation between Asn179 in P54 and Asp179 in the native structure. An alternate interaction occurs in P54 between Asn179 and Ala69, adjacent to the catalytic Ser70. This disorder affects catalysis since some of the disordered residues, in particular Glu166, form part of the active site. Stopped-flow kinetic measurements of native and P54 β-lactamase with nirocefin confirm the prediction that disordering of the catalytic Glu166 in P54 makes deacetylation the rate-limiting step in hydrolysis: whereas the ratio of the acylation rate to the deacylation rate is about 1 in native β-lactamase, in P54 this value is ~600, mainly due to the reduction in the deacetylation rate. The acylation rate is reduced about 10-fold. Thus, the kinetics of P54 support the proposal that the acylation and deacylation steps in β-lactamase are functionally separate and are assisted by different amino acid residues.

The structure of a class A β-lactamase (EC 3.5.2.6) from *Staphylococcus aureus* PC1 has been determined (Herzberg & Moult, 1987) and refined at 2.0-Å resolution (Herzberg, 1991), providing atomic details of the overall fold and the active-site architecture of the enzyme. The spatial disposition of key active-site residues suggests a catalytic pathway that shares some features with the serine protease family (Kraut, 1975). The overall fold of the molecule highlights an extensive loop segment [the Ω-loop involving residues 164-178 according to the numbering scheme of Ambler (1979) and Ambler et al., (1991)], part of which is involved in the formation of the active site. In particular, we have proposed that Glu166, located on the loop, plays a catalytic role in the deacylation of the enzyme. The packing of the Ω-loop against the rest of the structure is rather loose, with nine internal solvent molecules in between (the "cave"). In addition, a very unusual sterically strained cis peptide has been identified between the catalytic Glu166 and Ile167 located on the Ω-loop. These two features suggest that the loop may be marginally stable and readily undergoes conformational transition. Our structural observations can be linked to Pain's folding experiments (Robson & Pain, 1976a,b; Adams et. al., 1980; Mitchinson

† Supported by NIH Grant R01-AI27175 and by a NATO travel grant.
* To whom correspondence should be addressed.
‡ University of Maryland.
§ University of Edinburgh.

0006-2960/91/0430-9503$02.50/0